ANALYSES OF SPACE ENVIRONMENT EFFECTS ON ACTIVE FIBER OPTIC LINKS ORBITED ABOARD THE LDEF

E. W. Taylor, T. W. Monarski, J. N. Berry, A. D. Sanchez
R. J. Padden, and S. P. Chapman

AFSC Phillips Laboratory
Directorate of Space and Missiles Technology
Kirtland AFB, NM 87117-6008
Telephone: (505) 846-4741; FAX: (505) 846-2290

ABSTRACT

This analysis correlates the results of the "Preliminary Analysis of WL Experiment #701, Space Environment Effects on Operating Fiber Optic Systems," [Ref 1] with space simulated post retrieval terrestrial studies performed on the M0004 experiment. Temperature cycling measurements were performed on the active optical data links for the purpose of assessing link signal to noise ratio and bit error rate performance some 69 months following the experiment deployment in low Earth orbit. The early results indicate a high correlation between pre-orbit, orbit, and post-orbit functionality of the first known and longest space demonstration of operating fiber optic systems.

INTRODUCTION

The Air Force Systems Command (AFSC) Phillips Laboratory (PL) Experiment #701 (formerly Weapons Laboratory Experiment #701), also referred to as Experiment M0004, "Space Environment Effects on Fiber Optic Systems," [Refs 1,2,3] was deployed aboard the Long Duration Exposure Facility (LDEF) into space orbit by the shuttle *Challenger* on 6 April 1984. The experiment was positioned in tray location F8, 30° from the direction of the LDEF velocity vector, placing it close to the leading edge of the satellite. The LDEF was retrieved on 12 January 1990 by the shuttle *Columbia* after a nearly six year exposure to the adverse space environment elements of radiation, debris, micrometeorites, temperature cycling, and atomic oxygen scavenging.

The objective of the experiment was to measure the effects of the space environment on cabled fiber optics for correlation to previous extensive radiation effects studies performed nearly a decade ago [Ref 4-10]. End results on the effects of space debris and micrometeorite impacts as well as contamination experienced by the experiment space exposed surfaces have also been documented [Ref 11]. The intent of this paper is to report on the observed responses of three of four operational fiber optic links responding to orbital temperature cycling (the fourth link was not operational due to a micrometeorite or debris impact experienced after the first year in orbit). As a result, the loss of optical signal waveguiding resultant from temperature induced refractive index changes has been observed to various degrees in the three

EXPERIMENT NO. <u>M0004</u>

links. Radiation induced effects are reported elsewhere [Refs 1-3, 12, 13, 14]. Analysis on the losses in the individual components of each link is underway and will be reported in a later paper. However, the intent of this paper is to identify and bound the influence of the orbital temperature changes on the performance of links 1-3.

ANALYSES

Shown in Figure 1 is the experimental arrangement used to measure the operational performance of the optical fiber links during the first year of orbit. For the first six months in space, data was collected every six days, with the first measurement accomplished on the sixth day of orbit. During the last six months of orbit, data collection occurred every fourth day, totaling 76 measurements performed over the first year. Data collection and measurement, both in orbit and terrestrially, of several link parameters including signal to noise ratio (SNR), number of errors, types of errors, and temperature induced attenuation was accomplished using digital processing methods [Refs 1, 2, 3, 9].

In Figure 1, the experiment controller actuates a pseudo-random pulse generator and an error detector circuit which are switched successively between the four optical fiber links. A stream of 130,944 bits then passes through the link under measurement, and the processed signal is compared to the output of the pseudo-random generator. Any mismatch is considered an error as identified by Gilbert Statistics (Type I, II, and III) [Refs 6-7]. If the number of errors counted is less than 128 Type I errors, the counters are cleared, the threshold level of the detector comparator circuit is then incremented by + 1.25 mV, and another bit stream is sent through the link. When 128 or more independent (Type I) errors were detected, the experiment terminated the run, stored the data for use in the SNR determinations, and proceeded to exercise the next link in the measurement sequence.

The optical sources used to power the optical fibers in the experiment were light emitting diodes, three of which operated at a wavelength of 830 nm, while the fourth optical source operated at a wavelength of 1300 nm. Three of the optical fibers were plastic coated silica (PCS) step index fibers, while the fourth fiber operating at λ = 1300 nm was a semi-graded glass-glass fiber. Silica PIN photodiodes were used in the detection scheme. Analog temperature sensors (thermistors) were placed at different locations within the tray volume, and were read by an incrementing procedure using the digital to analog converter of Fig. 1, similar to the manner by which the threshold voltages were measured for each fiber link. The temperature resolution was determined to be within ± 0.1°C at room temperature (20°C) degrading to ± 2°C at the extremes of -80°C and + 150°C. It was over this range that the optical detector output was evaluated by the experiment comparator circuitry to determine the changes in the link threshold voltages. These changes representing the overall link performance over a one year period are shown in Fig. 2.

As shown in Figure 2, the orbital performance of the four optical fiber links was directly related to the temperature conditions internal and external to the tray. (While minimal radiation induced effects were also present, and the magnitude of the dose received was

measured, the results not included in this analysis are reported elsewhere [Refs 1-3].) The cyclic variation of the measured temperatures within the tray are attributed to the incident solar heat flux impinging the tray surface and conducting/radiating to the inner tray volume. Illustrated in Fig 3 is a comparison of an internal tray sidewall temperature measured by one of the experiment thermistors and the NASA THERM-Longeron 6 temperature [Ref 15]. The THERM data provided by NASA was also collected actively during spaceflight. Considering the two measurements were made several longerons apart, and are not the same time interval for t > 125 days, the measurements are in close agreement. The disagreement in orbital temperature data for t < 125 days is currently under investigation.

The large deviations in the optical signal levels observable in Figs 2a and 2b are believed due to the temperature induced loss of waveguiding in the fibers as previously reported [Refs 6-8]. The difference between the cladding region index (n_{cl}) and the core index (n_c) is given as $\Delta n = n_c - n_{cl}$. Due to the non-equivalent temperature induced index changes experienced by these regions, the fiber waveguiding efficiency decreases as n_c and n_{cl} change at different rates. Here, n_{cl} decreases rapidly at low temperatures. A re-polymerization phase process may occur in the cladding during low temperature cycling, leading to an optical transmission hysteresis phenomenon [Ref 6]. Of course, any radiation induced color center losses also add to the decrease in signal transmission, and the likelihood of temperature annealing of these defects is decreased significantly at low end temperatures [Ref 6-8]. Mechanical stress or bending effects can also cause the large deviations. Macro and microbending effects as a function of temperature can cause signal losses at lower temperatures. Also, fiber movement within the cabling due to thermal expansion and contraction can result in causing misalignments within the optical connectors which in turn can degrade the optical signal throughput.

Comparison of pre- and post-orbit absorption/emissivity (α/ϵ) measurements on the space-exposed panels of M0004 was conducted. There are two different paint colors on the exposed part of the tray: white and gray. The fiber plates were colored gray, and the rest of the exposed area was white. Pre-orbit measurements of α/ϵ were taken at four different places on the experiment, as shown in Fig 4. The α/ϵ measurements for those points are as follows: A = .55/.89, B = .70/.89, C = .70/.89, and D = .30/.85. It follows that A-C have similar values of α since they were all gray. Also, since point D is on a white panel, it should have a lower α than the adjacent gray panels. Following the experiment retrieval, α/ϵ measurements were taken again at Kennedy Space Center (KSC). However, measurements were not taken for points A-C so as not to disturb the exposed fiber cables. Thus a comparison can only be made at point D. Its post-orbit α/ϵ value was .32/.908. Thus, while there were changes in both the absorption and emissivity, the overall ratio only changed from 0.35 to 0.36. Since this α/ϵ measurement consisted of a different color than that of the other three, it is not assured that α/ϵ did not change at the other points. However, it appears that the exposed areas of the tray, and thus the fiber links which were in contact with those areas, experienced consistent temperature cycling throughout the duration of the spaceflight, and this point of view is assumed in the following analysis.

The experimental setup for the pre-orbit temperature measurements is shown in Fig 5. Sensors 2 and 3, which were attached to the back of the fiber plates, were averaged to get the temperature readings seen in Figure 6. Links 2 and 3 were fitted with ITT UNILUX/FOS connectors, while link 1 has Amphenol 906-110-5016 connectors. These were the connectors used during flight. The light source for all three links was a pigtailed RCA LED operating at $\lambda = 820$. The detector used was a UDT power meter. The data acquisition scheme was as follows for all links: start at room temperature; raise the oven temperature to 60°C; lower the temperature to -40°C; raise the temperature back to room temperature. Data was taken in a continuous manner. For convenience of comparison, the data was converted to illustrate optical signal attenuation in dB, where increased attenuation is shown in the negative y-direction.

During post-orbit testing, the fiber plate temperature measurements were made in a slightly different fashion. The major difference here was that data was collected by operating the experiment at different temperatures to obtain individual fiber link SNR values. These SNRs were converted into optical power, and then into attenuation. This approach was used to prevent fully de-integrating the fibers from the experiment, since follow-on investigations will be performed on the experiment. Another difference was the manner in which the temperature cycling was performed. For link 1, the starting point for the temperature measurements was room temperature; next, the temperature was lowered to -40°C; finally, the temperature was raised to 60°C. For links 2 and 3, the starting point was 60°C, with decreasing temperature points to -40°C. The different approaches were made based on pre-flight testing hysteresis information. The comparison between pre and post-orbit fiber link responses to temperature cycling can be viewed in Fig 6.

For link 1, there are some notable differences between the pre- and post-orbit data. First, the post orbit data showed an increase in performance at higher temperatures. But more importantly, at the lower temperatures, there was increased attenuation in the performance of the post-orbit data with respect to the temperature. Also, the slope of attenuation was greater than the pre-orbit data. While incrementally increasing the link temperature during post-orbit analysis, the link did not regain performance at the same point at which it was lost displaying hysteresis. It took another 10°C in temperature increase for this link to "turn on."

For link 2, the pre- and post-orbit data were somewhat similar. The major difference here was that the post-orbit data displayed near step function characteristics at 0°C (performance went from normal operating levels to an off state for a change of 10°C) while the pre-orbit data showed a gradual degradation in performance (performance went from normal operating levels to an off state in 60°C). Another difference was that the pre-orbit data showed a greater attenuation than the post-orbit data. But this is most likely a result of the data acquisition process of the experiment electronics. Specifically, when the SNR is determined for a given link, the initial threshold level is not set to zero signal output. Thus, it is not necessarily possible to obtain the minimum power level being detected by the receivers.

For link 3, the pre- and post-orbit data are very similar. Most notable is the close agreement between the pre- and post-orbit data, and the high performance of the link across

C-3

the entire temperature range. Also, there is a slight increase in performance at low temperatures for both the pre- and post-flight data.

Since the fiber used in links 2 and 3 are very similar in composition, but the performances of these links were rather different, an interesting conclusion can be drawn. The only difference between the two is that the cabling for link 2 is a loose tube configuration, while the cabling for link 3 was a tight conformal wrap. Thus it appears that the cabling of fiber optic links plays a major role in controlling temperature effects.

Another type of temperature cycling calibration was performed during the post orbit analysis. This calibration involved cooling the entire experiment tray, as experienced in space, rather than cooling the isolated fiber plate, as previously discussed in this paper. The purpose for doing this was two-fold. First, it was an attempt to correlate the entire tray temperature response with the orbital data. Second, it was an attempt to determine if temperature changes of the electronics (which only happened during the whole tray testing) had any effect on the performance of the links. The results of the fiber plate and entire tray testing were very similar, and thus the electronics were ruled out as being a cause of any of the temperature effects seen in performance in the orbit data. This is not unexpected, since the use of thermal blankets between the space exposed cover plates and the inner volume provided thermal insulation between the space exposed optical fibers and the experiment electronics, optical sources, and optical receivers. Our next analysis will use external sources and detectors to measure the effects of temperature cycling on the cabled optical fibers, thus removing any uncertainty introduced by the experiment A-D circuitry.

In conclusion, we have reported the first known data measuring the performance of step and graded-index optical fibers operating in a prolonged space environment under widely varying temperature conditions. It was observed that no permanent damage was experienced by either the glass or PCS optical fiber links due to the orbital temperature cycling experienced by the space exposed fibers. Also, it was shown that the cabling configuration plays a significant role in the control of temperature effects. While directly subjected to the harsh space environment, the cabled fibers and their optoelectronic components were recorded to operate, but were highly degraded at the low temperature extreme. Finally, it must be noted that the fibers which were subjected to the space environment are those of a much earlier generation technology. Considering the advances which have been made since the experiment was launched, newer generation fiber optics systems should be a reliable resource for use in space.

REFERENCES

[1] Taylor, E. W.; Berry, J. N.; Sanchez, A. D.; Padden, R. J.; and Chapman, S. P.: Preliminary Analysis of WL Experiment #701, Space Environment Effects on Operating Fiber Optic Systems. NASA Conference Publication 3134 *LDEF - 69 Months in Space - First Post Retrieval Symposium Part 3*. June 2-8, 1991.

[2] Taylor, E. W.; Berry, J. N.; Sanchez, A. D.; Padden, R. J.; and Chapman, S. P.: First Operational Space Fiber Optic Links Orbited Aboard the Long Duration Exposure Facility - Lessons Learned. *Proc. DoD Fiber Optics '92.* March 24-27, 1992. McLean, VA. pp. 25-28.

[3] Taylor, E. W.: Performance of the First Operable Fiber Optic Systems in Prolonged Space Orbit. *Proc. International Society for Optical Engineering.* Vol. 1691, Small Satellite Technologies and Applications. April 20-24, 1992.

[4] Taylor, E. W.: Fiber Optics Space Effects. *Proc. of Fiber Optics and Communication,* Sep. 1978, pp. 245-247.

[5] Taylor, E. W.: Some Recent Fiber Optics Research, Development and Applications Conducted by The Air Force. *Proc. Fiber Optics in the Nuclear Environment.* Vol 1: Applications. DNA 5308P-1, pp. 209-221, (May 1980).

[6] Taylor, E. W.; Emmes, J. M.; Barnes, C. E.; and Wiczer, F.: Behavior of Irradiated Plastic Clad Silica Fibers at Low Temperatures. *Photon 80 Conf. Proc.* Compte-Rendu, Paris, FR, pp. 110-117 (October 1980).

[7] Taylor, E. W.; Emmes, J. M.; Ayres, W. R.; Wiltse, J. D.; and Merritt, J. K.: Response of Irradiated Optical Waveguides at Low Temperatures. *Society of Photo-Optical Instrumentation Engineers,* Vol. 296, pp. 40-50 (August 1982).

[8] Taylor, E. W.; Myatt, L. J.; and Wiltse, J. D.: Low Temperature Gamma Irradiation of Polymer Coated Optical Waveguides. Presented at Photon 83, Paris, FR *Society of Photo Optical Instrumentation Engineers,* Vol. 404, pp. 55-59 (May 1983).

[9] Johnston, A. R.; Bergman, L. A.; and Taylor, E. W.: Fiber Optic Experiment For The Shuttle Long Duration Exposure Facility. *Society of Photo-Optical Instrumentation Engineers,* Vol. 296, pp. 40-50 (August 1982).

[10] Taylor, E. W.: Space Effects on Fiber Optics Systems. NASA SP-473, *The Long Duration Exposure Facility, Mission 1 Experiments,* edited by L. G. Clark et al., Washington, DC pp. 182-184 (1984).

[11] McKnight, D. S.; Dueber, R. E.; and Taylor, E. W.: Space Debris and Micrometeorite Events Experienced by WL Exp #701 In Prolonged Low-Earth Orbit. *J. Geophys. Res, Space Physics,* Vol. 96, No. A6, pp. 9829-9833, June 1, 1991.

[12] Taylor, E. W.: An Experiment for Studying Monolithic Integrated Optics Performance in the Space Environment. *SPIE Cambridge Symposium on Optical and Electro-optical Engineering, Integrated Optical Circuit Engineering II,* Vol. 548, pp. 46-50, September 1985.

[13] Benton, E. V.; and Heinrich, W.: Ionizing Radiation Exposure of LDEF. *USF-TR-77,* August 1990.

[14] Armstrong, T. W.; and Colborn, B. L.: Scoping Estimates of the LDEF Satellite Induced Radioactivity. *SAIC-90/1462,* September 1990.

[15] Bourassa, R. J.; and Gillis, J. R.: Solar Exposure of LDEF Experiment Trays. *NASA Contract Report 189554,* February 1992.

LIST OF INCLUDED FIGURES

Figure 1 : Configuration of Experiment Hardware

Figures 2a-2d : Orbital Performance Data on PL Exp #701

Figure 3 : Comparison of M0004 Thermistor 4 and LDEF THERM Longeron 6

Figure 4 : Location of pre- and post-orbit α/ϵ measurements

Figure 5 : Experimental Setup for terrestrial temp cycling and transmission measurements

Figure 6a : Comparison of pre- and post-orbit temp cycling on link #1.

Figure 6b : Comparison of pre- and post-orbit temp cycling on link #2.

Figure 6c : Comparison of pre- and post-orbit temp cycling on link #3.
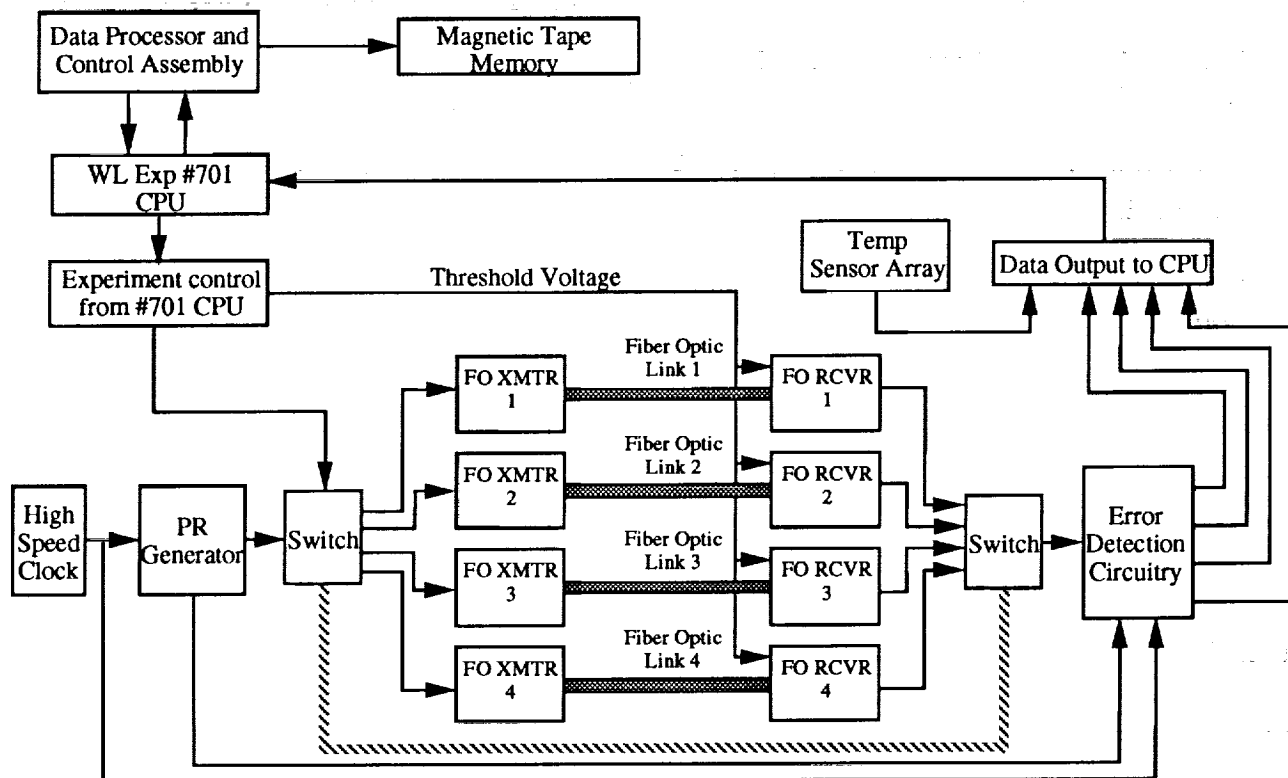
Figure 1. Configuration of experiment hardware. This hardware was used to measure the performance of the four active digital fiber optic links contained in PL Experiment #701 (M0004). The experiment measured the temperature at various locations within the tray volume and the performance of the fiber optic links by measuring the Signal-to-Noise Ratio and Bit-Error Rate of each link.
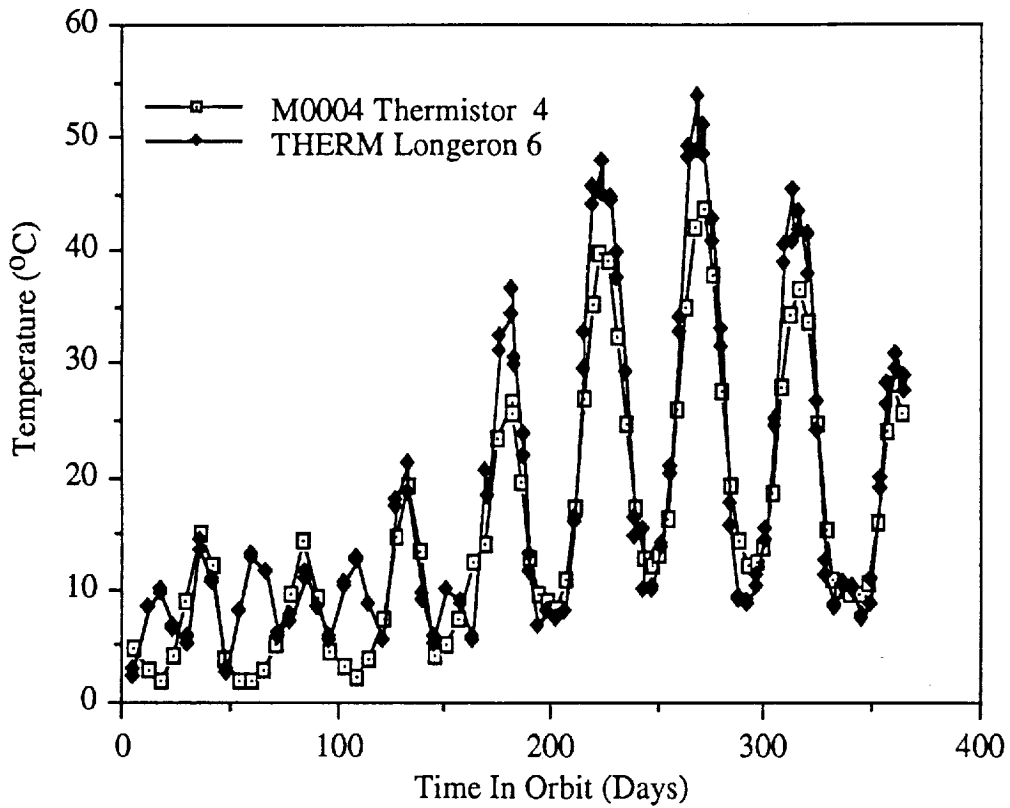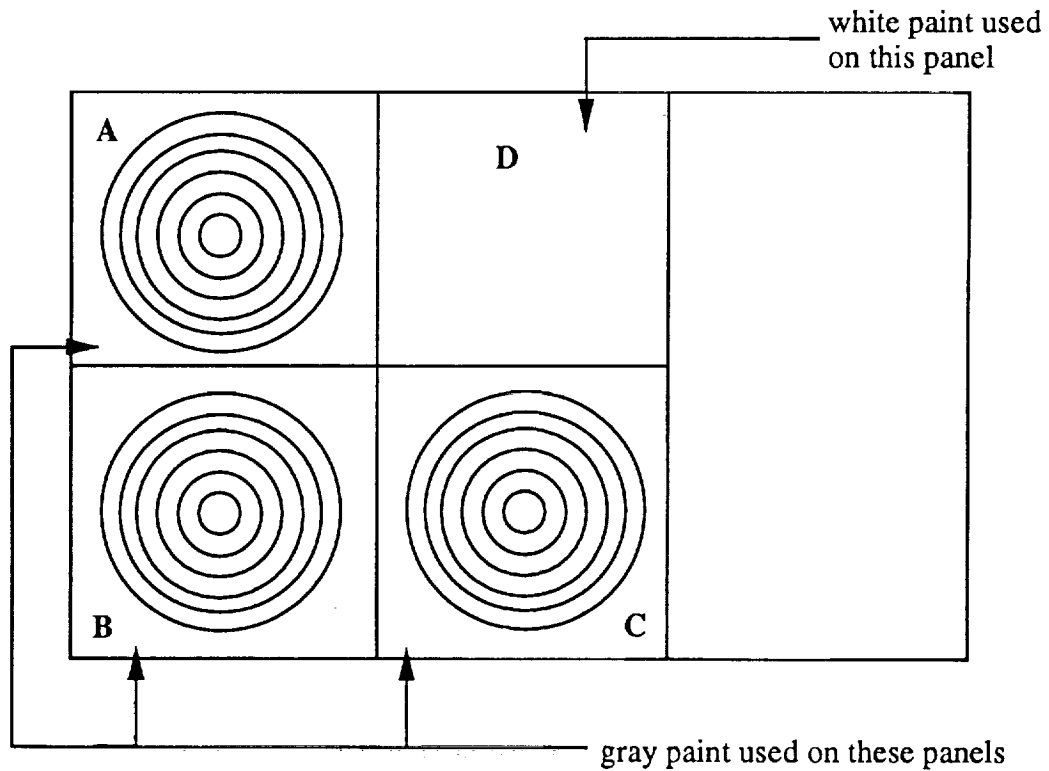
1432
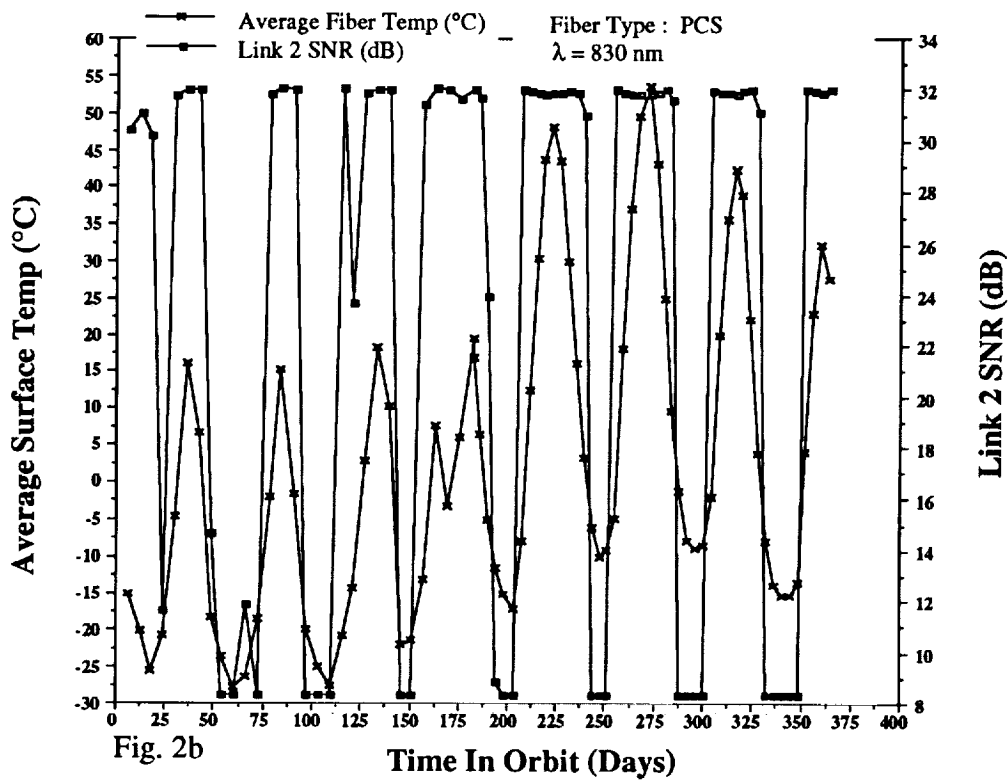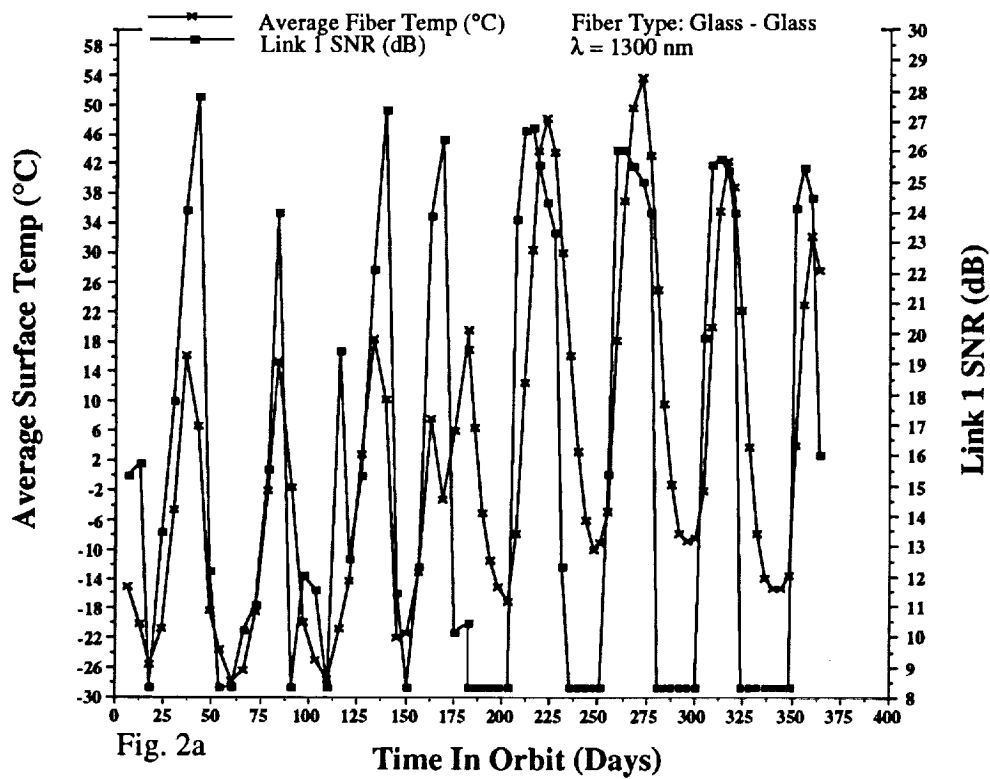
Figures 2a - 2b. Orbital performance data on PL Exp # 701 (M0004) Space Environment Effects on Fiber Optic Systems
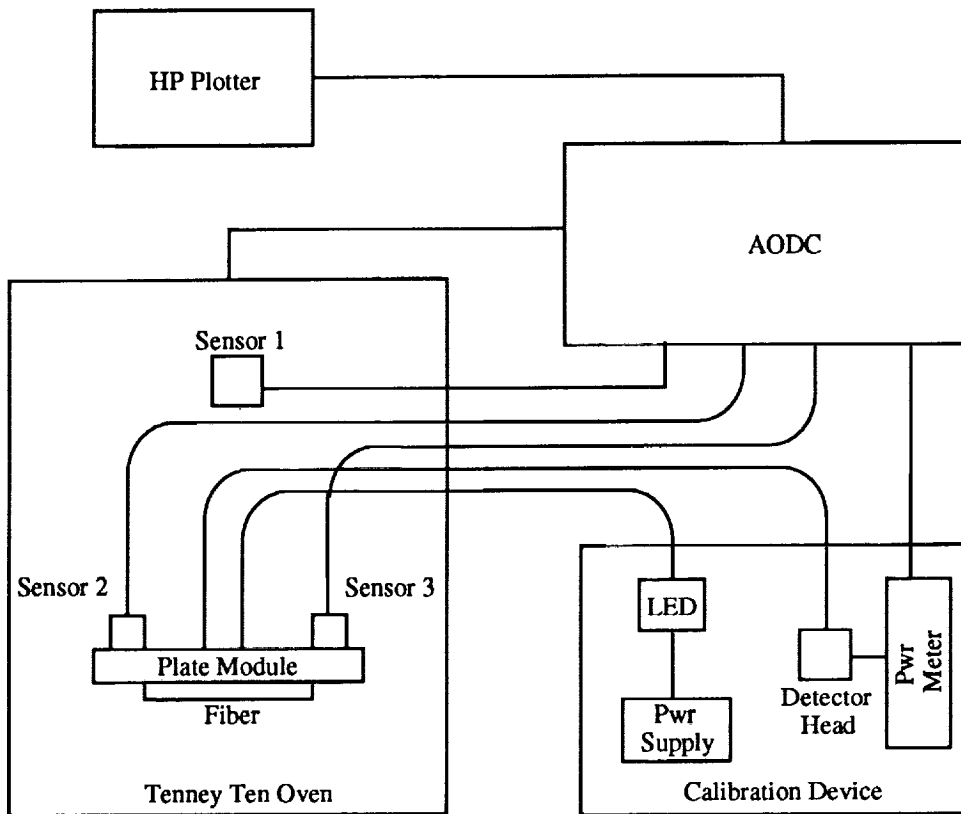
Fig. 2c

Fig. 2d
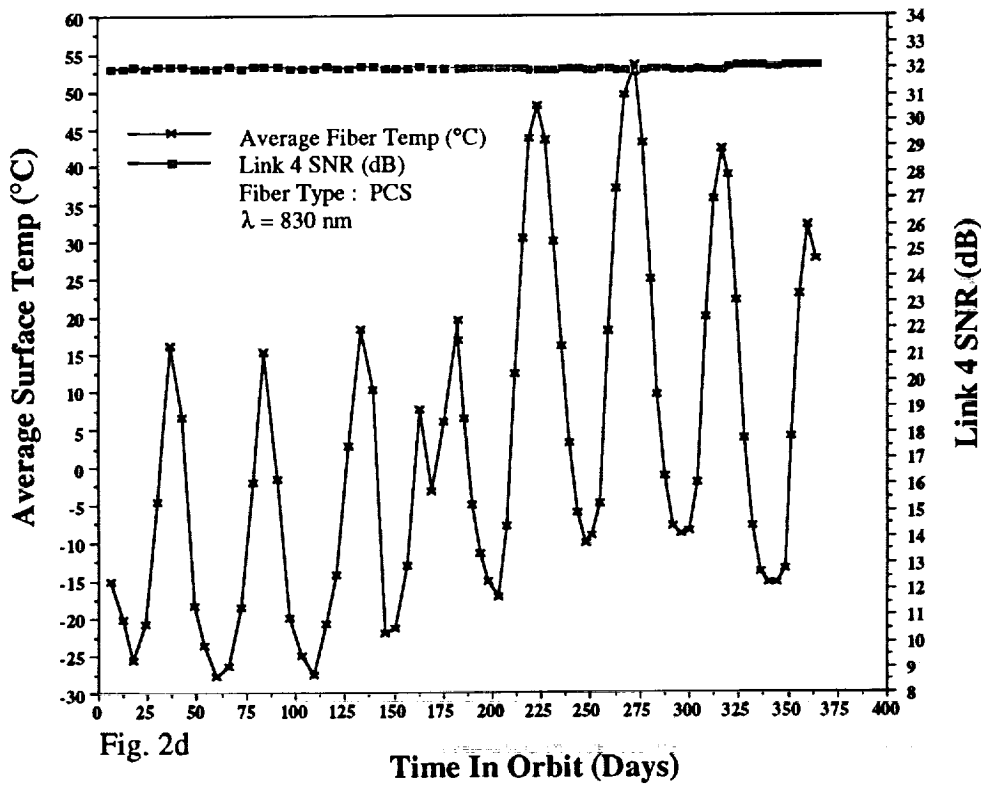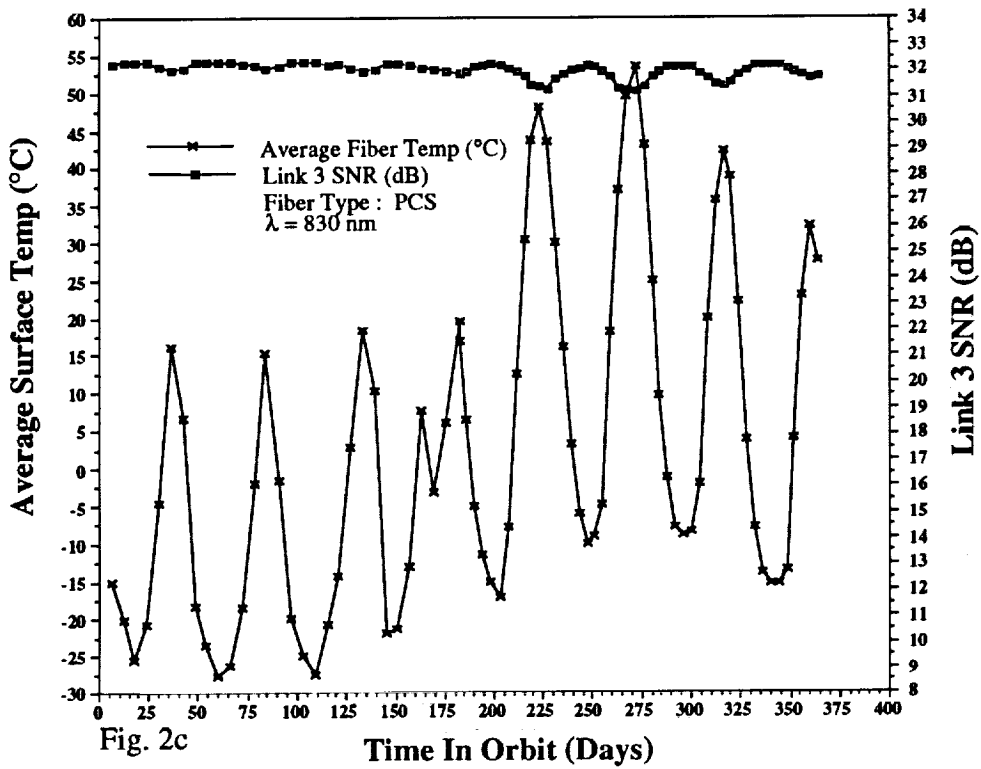
Figures 2c - 2d. Orbital performance data on PL Exp # 701 (M0004) Space Environment Effects on Fiber Optic Systems
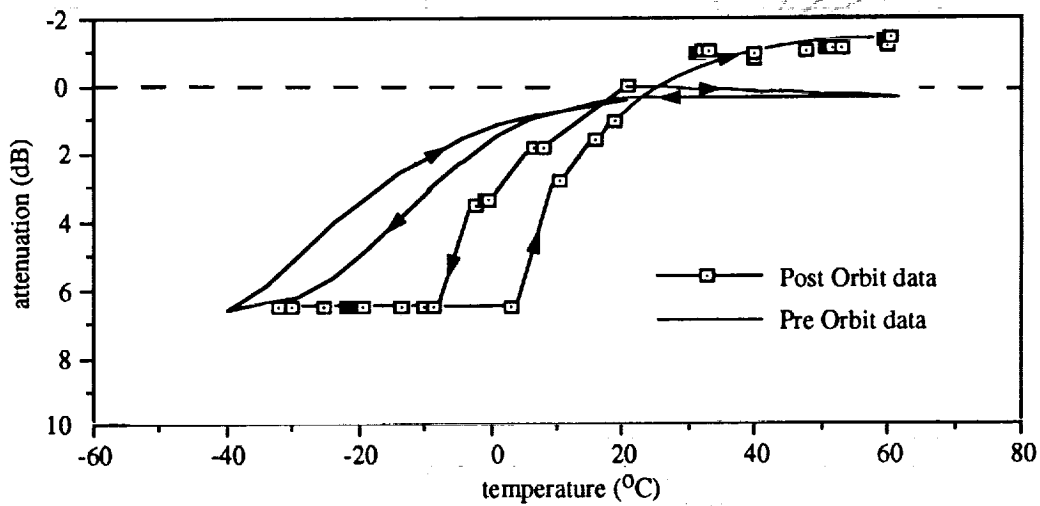
Figure 3. Comparison of M0004 Thermistor 4 and LDEF THERM Longeron 6 data. This comparison shows the good correlation between the two sets of orbit data.


**Figure 4.** Location of pre and post orbit α/ε measurements

Figure 5. Experimental set up for terrestial temperature cycling and transmission measurements

Figure 6a. Comparison of pre and post orbit temperature cycling on link #1. Here, signal attenuation occurs at a higher temperature for the post orbit data. Also, it can be observed that there is a greater degree of hysteresis in the post orbit data.
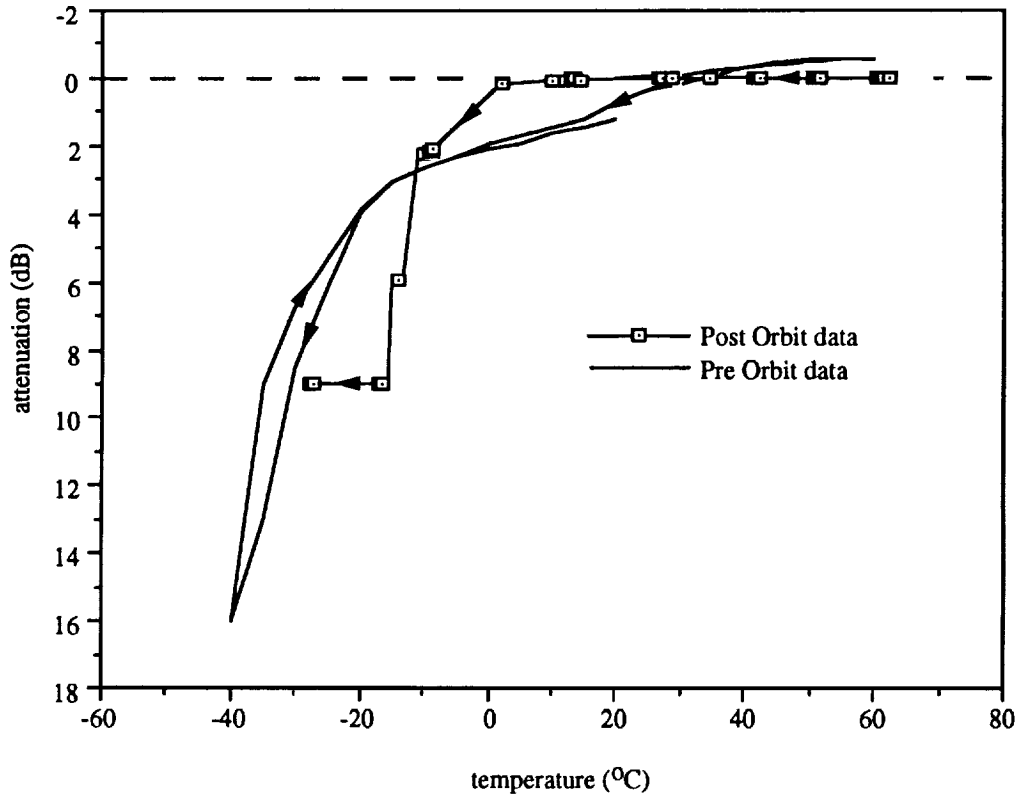
Figure 6b. Comparison of pre and post orbit temperature cycling on link #2. Although there is some correlation between pre and post orbit data, some subtle differences do exist. The "bottoming-out" of the attenuation for the post orbit data is most likely a result of the data acquisition process of the experiment electronics, and not a result of temperature cycling.
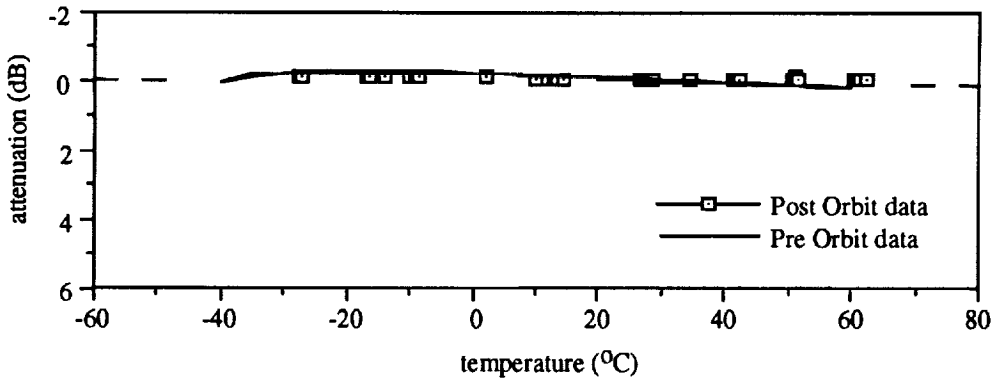
Figure 6c. Comparison of pre and post orbit temperature cycling on link #3. Here, the pre and post orbit correlation is excellent, and there is high link performance across the entire temperature range.